INTERNATIONAL JOURNAL OF COMMUNICATION SYSTEMS
Int. J. Commun. Syst. 2014; **27**:3383–3398
Published online 15 April 2013 in Wiley Online Library (wileyonlinelibrary.com). DOI: 10.1002/dac.2548

Compressive sensing for ultra-wideband channel estimation: on the sparsity assumption of ultra-wideband channels

Mehmet Başaran[1], Serhat Erküçük[2,*,†] and Hakan Ali Çırpan[1]

[1]*Department of Electronics and Communications Engineering, Istanbul Technical University, Maslak 34469, İstanbul, Turkey*
[2]*Department of Electrical and Electronics Engineering, Kadir Has University, Fatih 34083, İstanbul, Turkey*

SUMMARY

Due to the sparse structure of ultra-wideband (UWB) multipath channels, there has been a considerable amount of interest in applying the compressive sensing (CS) theory to UWB channel estimation. The main consideration of the related studies is to propose different implementations of the CS theory for the estimation of UWB channels, which are assumed to be sparse. In this study, we investigate the *suitability of standardized UWB channel models* to be used with the CS theory. In other words, we question the *sparsity assumption* of realistic UWB multipath channels. For that, we particularly investigate the effects of IEEE 802.15.4a UWB channel models and the selection of channel resolution both on channel estimation and system performances from a practical implementation point of view. In addition, we compare the channel estimation performance with the Cramer-Rao lower bound for various channel models and number of measurements. The study shows that although UWB channel models for residential environments (e.g., channel models CM1 and CM2) exhibit a sparse structure yielding a reasonable channel estimation performance, channel models for industrial environments (e.g., CM8) may not be treated as having a sparse structure due to multipaths arriving densely. Furthermore, it is shown that the sparsity increased by channel resolution can improve the channel estimation performance significantly at the expense of increased receiver processing.

Received 19 June 2012; Revised 27 November 2012; Accepted 6 March 2013

KEY WORDS: compressive sensing (CS); ultra-wideband (UWB) channel estimation; IEEE 802.15.4a channel models; channel resolution

1. INTRODUCTION

There has been a great interest in ultra-wideband (UWB) impulse radio (IR) systems as they can operate with low transmit power, have low cost simple transceiver structures, and the received signal is rich in multipath diversity with fine time resolution [1]. As a result of these properties, UWB-IR systems have been selected as the physical layer structure of the wireless personal area network (WPAN) standard IEEE 802.15.4a for location and ranging, and low data rate applications [2]. Specifically, the fine time resolution property of UWB signals at the receiver has made it an important candidate in angle of arrival estimation and direction finding [3]. In addition to location and ranging studies, there have been interest in exploiting the UWB system performance [4] and channel capacity [5]. Although the main interest in these studies is to improve the system performance or increase the channel capacity, UWB systems should also exhibit low cost and low power implementation structures. Accordingly, time reversal and transmitted reference techniques have been considered to reduce processing at the receiver or to effectively avoid channel estimation at

*Correspondence to: Serhat Erküçük, Department of Electrical and Electronics Engineering, Kadir Has University, Fatih 34083, İstanbul, Turkey.
†E-mail: serkucuk@khas.edu.tr

the expense of performance loss. In [6], an indoor UWB communication system that applies time reversal for transmitting UWB pulses is proposed. In [7], transmitted reference pulses are considered for multiple access. Although transmitted reference techniques do not use user channel information and perform poorly [7], most other approaches (e.g., [1, 3–6]) need accurate channel estimation to achieve the desired system performances.

For the channel estimation of UWB-IRs, the conventional maximum-likelihood (ML) channel estimation approach has been widely considered and adopted [8, 9]. The main drawback of the implementation of an ML estimator is that very high sampling rates are required for accurate channel estimation due to the extremely wide bandwidth of the UWB-IRs (at least 500 MHz). This contradicts with the low cost and low power implementation purpose of UWB-IRs. Because of the emerging framework of compressive sensing (CS) [10, 11], there has been a growing interest in applying the CS theory to sparse channel estimation [12, 13]. As the UWB-IR signals have resolvable multipaths with a sparse structure at the receiver, the application of CS theory to UWB channel estimation has also found wide interest in the UWB community. Recently, the main interest in UWB-IR system design is to reduce the receiver complexity and implementation cost [14]. Accordingly, two relatively new research topics have emerged: CS-based UWB transceiver design and CS-based UWB channel estimation. For the CS-based transceiver design, the main goal is to detect the UWB signal with reduced sampling rate and yet with negligible performance degradation [15–17]. For the CS-based channel estimation, the main goal is to estimate the sparse channel with reduced number of observations [18–24].

The related CS-based UWB channel estimation studies can be summarized as follows. One of the first applications of CS theory to UWB channel estimation can be found in [18]. In that study, signal reconstruction and channel estimation methods based on the matching pursuit (MP) algorithm were proposed. Although the paper mainly focused on the details of the MP algorithm, the authors provided only reconstruction error curves and BER curves. However, channel coefficient estimation errors were not provided, which are important in determining the channel estimation performance. In [19], the authors combine the ML approach with the CS theory. The simulation based study shows that the combined CS–ML method can outperform the MP implementation at the expense of increased complexity. It should be noted that the conventional MP performances provided in the paper even for the best case (i.e., at 20 dB signal-to-noise ratio (SNR)) were close to unity, which is quite high for practical MP implementation. In [20], the authors consider pre-modulating the UWB signal with a spread spectrum sequence followed by random sampling in the Fourier domain. They compare the SNR of the reconstructed signal with other sampling methods such as random Fourier sampling and Gaussian measurements. They claim that their proposed method outperforms other sampling methods in terms of SNR. Despite the claimed advantage in terms of SNR, their implementation does not account for the exact multipath locations and amplitudes, which are very important for channel estimation implementation. In [21], a pre-filtering method has been proposed so as to replace the measurement matrix. The authors claim that their proposed pre-filter can effectively suppress noise. However, the paper lacks clarity in presenting the comparative results as they do not provide any channel coefficient estimation error plots and only present BER curves with bit errors in the order 10^{-5} at very low SNR values. Although the relative performance results provided may be correct, the exact performances should be revised for clarity. In [22], the authors update the measurement matrix adaptively using the information of the energy distribution of the received pilot signal in each frame and use the method of distributed CS (DCS) to get the channel estimate. They use this model to modify the orthogonal MP (OMP) algorithm. Although the authors present improved performance curves over the conventional OMP method, they use linear scale instead of the log scale; hence, possible gains at higher SNR regions cannot be determined clearly. In [23], MP and basis pursuit denoising (BPDN) techniques have been considered, and the channel estimates generated by these algorithms were used in correlation-based CS detectors to compare with transmitted reference system performance results. The authors present the system model of both channel estimation and data detection in the presence of inter-symbol interference, however, only present BER curves for comparison. Their results show that BPDN reconstruction outperforms TR and MP techniques in terms of the BER performance. In [24], the authors consider the frequency domain equivalent of sparse UWB channels and propose a greedy algorithm named extended OMP (eOMP)

DOI: 10.1002/dac

to reduce false path detection achieved with conventional OMP. Although the proposed method improves the OMP time-of-arrival estimation by reducing the false path detection probability, the authors do not present BER performance curves for the estimated channels and compare them with perfectly known channels. The main goal of the previous studies (i.e., [18–24]) is that they focus on improving the channel estimation and system performances based on the condition that UWB channels are sparse. The *sparse channel assumption* is widely accepted because of the properties of UWB signaling, which are (i) the transmission of low duty cycle pulses in the order of nanosecond duration, and (ii) the nanosecond duration pulses coming from different multipaths being individually resolved at the receiver. However, depending on the environment (e.g., an industrial environment may have dense multipaths) and the channel resolution (e.g., pulses may be different duration), the sparsity assumption of UWB channels may not hold. Therefore, this condition should be investigated in detail before CS can be applied to UWB channel estimation. Furthermore, most studies in the literature do not provide lower bounds for their channel estimation approach. However, this is a necessary consideration for any channel estimation implementation.

Motivated by these conditions, we investigate[‡] the *suitability of standardized UWB channel models* to be used with the CS theory. In other words, we question the sparsity assumption of realistic UWB multipath channels. For that, we particularly investigate the effects of two factors on the channel estimation performance from a practical implementation point of view: (i) the IEEE 802.15.4a UWB channel models, which are classified according to the measurement environments [25], and (ii) the selection of channel resolution, which depends on the transmitted pulse width, T_s, and determines the equivalent approximate T_s-spaced channel model [26]. Accordingly, the channel estimation performance is determined in terms of the mean square error (MSE) of the channel gain estimates, and the BER performance is investigated with the estimated channel parameters for various rake receiver implementations. The MSE and BER performances are discussed considering the effects of different system parameters. In addition, the channel estimation performance is compared with the Cramer-Rao lower bound (CRLB) for various channel models and number of measurements. The results of this study are important for the practical implementation of the CS theory to UWB channel estimation.

The rest of the paper is organized as follows. In Section 2, the CS theory and its application to channel estimation are presented. In Section 3, modeling the UWB channel according to the IEEE 802.15.4a channel models and the channel resolution are explained. In Section 4, simulation results for both the channel estimation performance and the system performance are presented. Concluding remarks are given in Section 5.

2. CS FOR UWB CHANNEL ESTIMATION

Compressive sensing theory introduced in [10, 11] has shown that a sparse signal can be recovered with high probability from a set of small number of random linear projections. In the following, the overview of the CS theory, how it can be applied to sparse UWB channel estimation, and the CRLB for the CS-based UWB channel estimation are presented, respectively.

2.1. Compressive sensing overview

Suppose that $\mathbf{y} \in \Re^N$ is a discrete-time signal that can be represented in an arbitrary basis $\mathbf{\Psi} \in \Re^{N\times N}$ with the weighting coefficients $\mathbf{x} \in \Re^N$ as

$$\mathbf{y} = \mathbf{\Psi}\mathbf{x}. \tag{1}$$

Suppose $\mathbf{x} = [x_1, x_2, \ldots, x_N]^{\mathrm{T}}$ has M nonzero coefficients, where $M << N$. By projecting $\mathbf{y}$ onto a random measurement matrix $\mathbf{\Phi} \in \Re^{K\times N}$, a set of measurements $\mathbf{z} \in \Re^K$ can be obtained as

$$\mathbf{z} = \mathbf{\Phi}\mathbf{\Psi}\mathbf{x} \tag{2}$$

[‡]Part of this work was presented at the IEEE International Conference on Ultra Wideband in Bologna, Italy in September 2011.

DOI: 10.1002/dac

where $K << N$. Instead of using the N-sample $\mathbf{y}$ to find the weighting coefficients $\mathbf{x}$, K-sample measurement vector $\mathbf{z}$ can be used. Accordingly, $\mathbf{x}$ can be estimated as

$$\hat{\mathbf{x}} = \arg\ \min \|\mathbf{x}\|_1 \quad \text{subject to} \quad \mathbf{z} = \mathbf{\Phi}\mathbf{\Psi}\mathbf{x} \tag{3}$$

where ℓ_p-norm is defined as $\|\mathbf{x}\|_p = \left(\sum_{n=1}^{N} |x_n|^p\right)^{1/p}$. Note that, the advantage of estimating $\mathbf{x}$ from the vector $\mathbf{z}$ instead of $\mathbf{y}$ is that the former having much fewer samples corresponds to a much lower sampling rate at the receiver. In addition to ℓ_1-minimization solution, there exists other greedy algorithm based solutions [10, 11, 18]. However, we focus our study on only ℓ_1-minimization as we are interested in relative performances for different channel models and resolutions for a selected CS method. We will now present how the CS theory can be used for UWB channel estimation.

2.2. Application of CS theory to UWB channel estimation

The CS theory explained in (1)–(3) can be applied to UWB channel estimation. Suppose that $\mathbf{r} \in \Re^N$ is the discrete-time representation of the received signal given as

$$\mathbf{r} = \mathbf{P}\mathbf{h} + \mathbf{n} \tag{4}$$

where $\mathbf{P} \in \Re^{N \times N}$ is a scalar matrix representing the time-shifted pulses, $\mathbf{h} = [\alpha_1, \alpha_2, \ldots, \alpha_N]^{\mathrm{T}}$ are the channel gain coefficients, and $\mathbf{n}$ are the additive white Gaussian noise terms. Because the UWB channel structure is sparse, $\mathbf{h}$ has only M nonzero coefficients. Similar to (2), the received signal $\mathbf{r}$ can be projected onto a random measurement matrix $\mathbf{\Phi} \in \Re^{K \times N}$ so as to obtain $\mathbf{z} \in \Re^K$ as

$$\begin{aligned} \mathbf{z} &= \mathbf{\Phi}\mathbf{P}\mathbf{h} + \mathbf{\Phi}\mathbf{n} \\ &= \mathbf{A}\mathbf{h} + \mathbf{v}\,. \end{aligned} \tag{5}$$

Due to the presence of the noise term $\mathbf{v}$, the channel $\mathbf{h}$ can be estimated as [27]

$$\hat{\mathbf{h}} = \arg\ \min \|\mathbf{h}\|_1 \quad \text{subject to} \quad \|\mathbf{A}\mathbf{h} - \mathbf{z}\|_2 \leqslant \epsilon \tag{6}$$

where the value of the parameter ϵ accounts for the noise power and can be represented as $\epsilon \geqslant \|\mathbf{v}\|_2$. This implies that the solution of (6) requires $\mathbf{z} - \mathbf{A}\mathbf{h}$ to be within the noise level [27]. Although the minimization problem in (3) can be modeled as a linear program and solved using generic path-following primal-dual method, the minimization problem in (6) can be recast as a second-order cone program and solved[§] with a generic log-barrier algorithm [28]. Considering (6), the channel estimation performance depends on the sparsity of $\mathbf{h}$ (i.e., the value of M), as well as the number of observations K. It is therefore necessary to understand the discrete-time equivalent structure of $\mathbf{h}$ by considering the effects of standardized channel models and channel resolution. In Section 3, we will elaborate on these effects. Next, we present the theoretical lower bounds for CS-based channel estimation.

2.3. Theoretical lower bounds for CS-based UWB channel estimation

There are many different channel estimation methods to model the communication environment (i.e., to identify the communication channel). To understand how close the estimation performance is to the best achievable performance for specified conditions, some lower bounds are defined. Accordingly, the CRLB can be used for this purpose, where the variance of the channel estimation error is bounded by the inverse of the Fisher information matrix. The CRLB for CS-based channel estimation can be obtained as in [29],

$$\text{CRLB} = \sigma_n^2 \cdot \text{trace}\left\{\left(\mathbf{A}_M^{\mathrm{T}}\mathbf{A}_M\right)^{-1}\right\} \tag{7}$$

[§]For the implementation of (6), the codes provided by Candes and Romberg publicly available at http://users.ece.gatech.edu/~justin/l1magic/ are used.

DOI: 10.1002/dac

where σ_n^2 is the additive white Gaussian noise variance and $\mathbf{A}_M \in \Re^{KxM}$ is a submatrix of $\mathbf{A}$ obtained by taking the columns of $\mathbf{A}$ corresponding to the indices of the nonzero components of the sparse channel vector $\mathbf{h}$. This performance indicator assumes that the receiver knows the locations of multipath components. Because the CS-based channel estimator does not know the multipath locations, inherently the previous CRLB is expected to be significantly better than the CS-based estimation performance. The computation of CRLB may not be trivial due to the computation of the inverse of the MxM matrix given in (7). Hence, we also consider the deterministic lower MSE (DL-MSE) as given in [30], which assumes to know multipath locations and serves as an approximation to (7). The deterministic lower MSE can be expressed as

$$E\left[\|\mathbf{h}^* - \mathbf{h}\|_2^2\right] \geqslant \frac{M}{K}\frac{1}{SNR} \tag{8}$$

where M is the number of nonzero components in the sparse channel vector $\mathbf{h}$, K is the number of observations, SNR denotes signal-to-noise ratio, and $\mathbf{h}^*$ is an oracle estimator that knows the multipath locations [30]. In Section 4, we will compare the MSE performances of the estimator and the two MSE lower bounds given in (7) and (8).

3. MODELING THE UWB CHANNEL

In this section, we specifically focus on the UWB channel structure. We initially present the UWB channel models followed by the channel resolution so as to model the discrete-time channel $\mathbf{h}$. We finally present the performance criteria to assess the effects of channel estimation performance.

3.1. Channel models

Most of the CS-based UWB channel estimation studies assume that the UWB channels are sparse. However, this is a vague assumption. To classify a channel as sparse, initially the channel environment should be examined. In [25], members of the IEEE 802.15.4a standardization committee have developed a comprehensive standardized model for UWB propagation channels. Accordingly, they have considered different environments and have conducted measurement campaigns to model the UWB channels for each environment. The channel environments that they have parameterized include indoor residential, indoor office, outdoor, industrial environments, agricultural areas, and body area networks. The details of the related channel models and their associated parameters can be found in [25]. We motivate our study with the selection of a variety of environments having either a line-of-sight (LOS) or a non-LOS (NLOS) transmitter-receiver connection. Accordingly, we select the CM1 (LOS indoor residential), CM2 (NLOS indoor residential), CM5 (LOS outdoor), and CM8 (NLOS industrial) channel models, which are widely used in UWB research.

Before we elaborate on each channel model, let us present the general channel impulse response (CIR) model. The continuous-time channel $h(t)$ can be modeled as

$$h(t) = \sum_{m=1}^{L_r} h_m \delta(t - \tau_m) \tag{9}$$

where h_m is the mth multipath gain coefficient, τ_m is the delay of the mth multipath component, $\delta(\cdot)$ is the Dirac delta function, and L_r is the number of resolvable multipaths. More discussions will be given on L_r when we discuss channel resolution in the next subsection. We summarize the characteristics of channel models CM1, CM2, CM5, and CM8 in Table I.

Using the CIR model in (9) and the parameters for channel models CM1, CM2, CM5, and CM8 in [25], a realization for each channel model is plotted in Figure 1.

DOI: 10.1002/dac

Table I. UWB channel models.

Channel model	Characteristics
CM1	This is by far the most commonly used channel model to assess the system performance. It models an LOS connection in an indoor residential environment. It is the most sparse channel model where few rake fingers can collect considerable amount of signal energy.
CM2	This is a channel model with an NLOS connection in an indoor residential environment. It complements CM1. It is a sparse channel model but usually contains more multipaths compared with CM1.
CM5	This is a channel model with an LOS connection in an outdoor environment. Typically, the multipaths arrive in a few clusters.
CM8	This is a channel model with an NLOS connection in an industrial environment. The multipaths arrive densely so that the channel does not have a sparse structure.

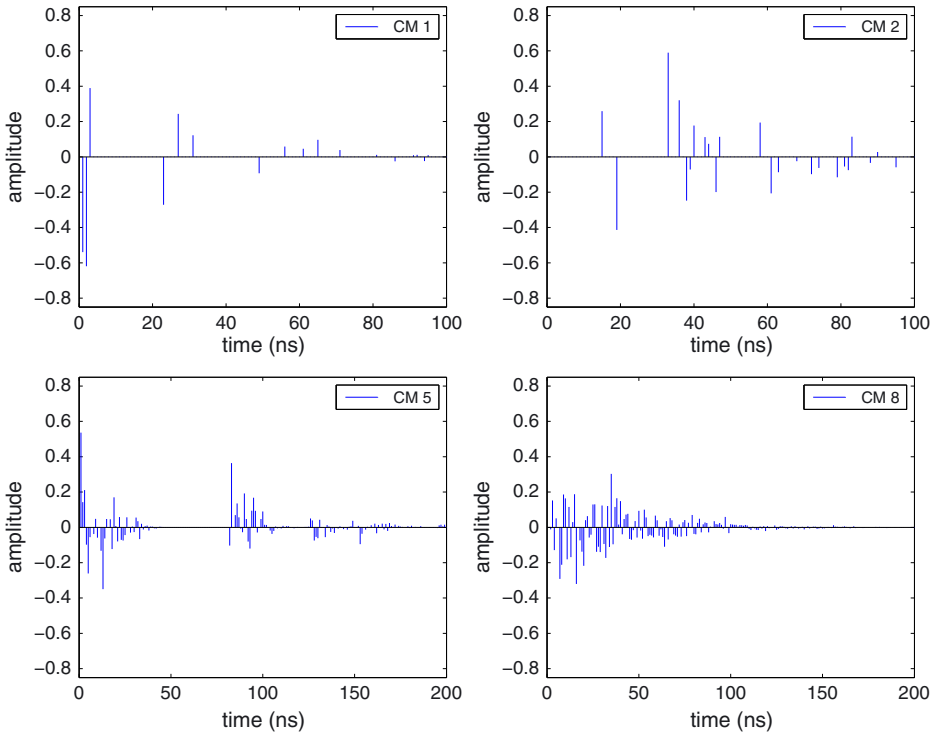

Figure 1. Channel realizations for CM1, CM2, CM5, CM8.

It can be observed that the typical channel properties listed in Table I can be observed in the figure. Next, we present how to obtain the discrete-time equivalent of (9) so as to use in (4)–(6).

3.2. *Channel resolution*

The continuous-time CIR given in (9) assumes that the multipaths may arrive any time. This is referred to as the τ-spaced channel model [26]. Suppose that two consecutive multipaths with delays τ_k and τ_{k+1} arrive very close to each other. Further suppose that a pulse of duration T_s is to be transmitted through this channel. If $T_s > |\tau_{k+1} - \tau_k|$, then the pulse at the receiver cannot be resolved individually for each path, and experiences the combined channel response of the kth and $(k+1)$th paths. Let us define an approximate T_s-spaced channel model that combines multipaths arriving in the same time bin, $[(n-1)T_s, nT_s]$, $\forall n$. Accordingly, for $[(n-1)T_s, nT_s]$, $\forall n$, the delays $\{\tau_m | 1, 2, \ldots, L_r\}$ that arrive in the corresponding quantized time bins can be determined, and the associated $\{h_m | 1, 2, \ldots, L_r\}$ gains can be linearly combined to give the new channel coefficients $\{\alpha_n | 1, 2, \ldots, N\}$. Note that some of the $\{\alpha_n\}$ values may be zero due to no arrival during that

DOI: 10.1002/dac

time bin, hence, the number of nonzero coefficients M satisfies the condition $M \leqslant L_r \leqslant N$. The equivalent T_s-spaced channel model can be expressed as

$$h(t) = \sum_{n=1}^{N} \alpha_n \delta(t - nT_s) \tag{10}$$

where $T_c = NT_s$ is the channel length. Using (10), the discrete-time equivalent channel can be written as

$$\mathbf{h} = [\alpha_1, \alpha_2, \ldots, \alpha_N]^{\mathrm{T}} \tag{11}$$

where the channel resolution is T_s. The discrete-time equivalent channel vector obtained previously then can be used in (4)–(6) in the context of CS theory.

The effect of channel resolution (i.e., selection of T_s) on the sparsity of the channel vector can be explained as follows. Let there be L_r nonzero multipath coefficients in the continuous-time channel $h(t)$ with channel length T_c. Let the two discrete-time equivalent channels with a channel resolution T_{s_1} have M_1 nonzero terms out of $N_1 = T_c/T_{s_1}$ coefficients, and with a channel resolution T_{s_2} have M_2 nonzero terms out of $N_2 = T_c/T_{s_2}$ coefficients, respectively. If $T_{s_1} < T_{s_2}$ (i.e., T_{s_1} has finer resolution), then $L_r \geqslant M_1 \geqslant M_2$ and $N_1 > N_2$. This is illustrated in Figure 2 for the $T_c = 30$ ns duration of a channel model CM1 realization. Although there are $L_r = 12$ paths in the τ-spaced channel model, the equivalent discrete-time model with $T_s = 0.5$ ns has $N_1 = 60$ samples of which $M_1 = 11$ of them are nonzero. On the other hand, if T_s is increased to 2 ns, then the channel has $N_2 = 15$ samples of which $M_2 = 9$ of them are nonzero. The remarks (A) and (B) shown on the

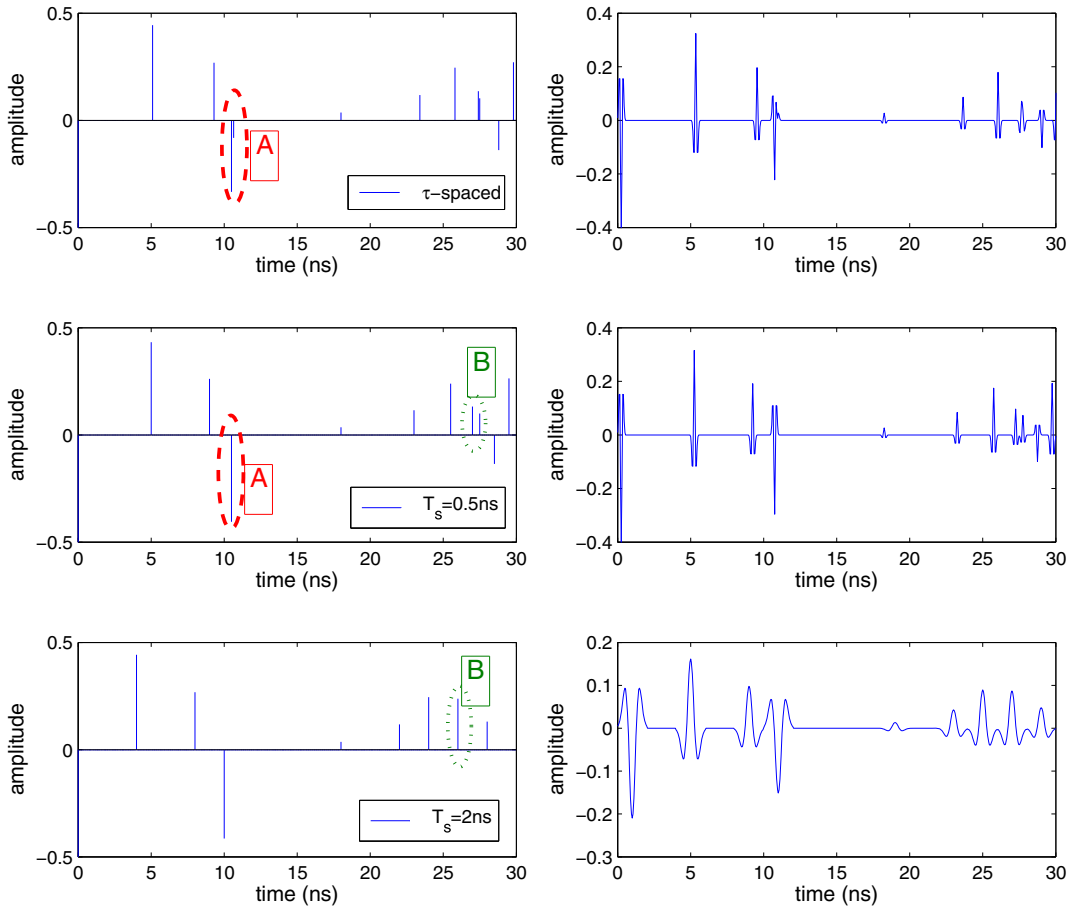

Figure 2. Discrete-time channel models with different channel resolutions.

DOI: 10.1002/dac

Table II. The sparsity ratios for different channel resolutions.

Channel model	$T_s = 1$ ns M/N	$T_s = 0.5$ ns M/N	$T_s = 0.25$ ns M/N
CM1	0.30	0.17	0.09
CM2	0.34	0.20	0.11
CM5	0.81	0.69	0.52
CM8	1.00	0.99	0.99

figure illustrate how the paths merge if they arrive in the same time bin for a given channel resolution so as to decrease L_r. We can also observe that if the channel resolution is finer, the channel will be sparser. In addition to these, the received signals are shown on the right hand side of the figure's columns when a pulse with T_s-duration is transmitted over the related channel.

Before explaining the receiver structure, we finally define the sparsity ratio (M/N) as the ratio of the number of nonzero coefficients (M) to the length of the discrete-time equivalent channel (N) for the selected resolution. We present in Table II the sparsity ratio, at various channel resolution values for different channel models obtained by averaging over 100 channel realizations when the channel length is fixed to $T_c = 100$ ns.

From the table, it can be deduced that the multipaths for CM5 and CM8 arrive very densely compared with CM1 and CM2; hence, even at the increased channel resolution (i.e., when T_s is decreased), the sparsity of these channels does not improve much.

3.3. Performance criteria

In communication systems, the performance of channel estimation is evaluated via MSE of the channel coefficients, and the overall system performance is assessed on the basis of BER.

3.3.1. Mean square error. Mean square error term is calculated as

$$MSE = \sum_{i=1}^{N} (\alpha_i - \hat{\alpha_i})^2 \tag{12}$$

where $\{\alpha_i\}$ are the channel coefficients as given in (11), and $\{\hat{\alpha_i}\}$ are the channel coefficient estimates obtained from (6).

3.3.2. Bit-error rate. Assuming binary phase shift keying modulation, the discrete-time received signal can be represented as

$$\mathbf{r} = d\mathbf{P}\mathbf{h} + \mathbf{n} \tag{13}$$

where $d \in \pm 1$ is the transmitted binary information. The decision statistic is determined by

$$D = \hat{\mathbf{h}}^{\mathrm{T}} \mathbf{P}^{-1} \mathbf{r} \tag{14}$$

and the data is estimated as

$$\hat{d} = \begin{cases} +1, & D \geqslant 0 \\ -1, & D < 0 \end{cases} \tag{15}$$

where $\hat{\mathbf{h}}$ and $\hat{d}$ are the estimated channel and data, respectively. For data estimation, if an all-rake receiver is used, $\hat{\mathbf{h}} = \hat{\mathbf{h}}_{AR} = [\hat{\alpha}_1, \hat{\alpha}_2, \ldots, \hat{\alpha}_N]^{\mathrm{T}}$ will give the best BER performance at the expense of increased complexity. For practical implementations, if a partial-rake with L fingers is used, $\hat{\mathbf{h}} = \hat{\mathbf{h}}_{PLR} = [\hat{\alpha}_1, \hat{\alpha}_2, \ldots, \hat{\alpha}_L, 0, \ldots, 0]^{\mathrm{T}}$, and if a selective-rake with L fingers is used, $\hat{\mathbf{h}} = \hat{\mathbf{h}}_{SLR}$ with the strongest L paths selected and the other coefficients equal to zero.

DOI: 10.1002/dac

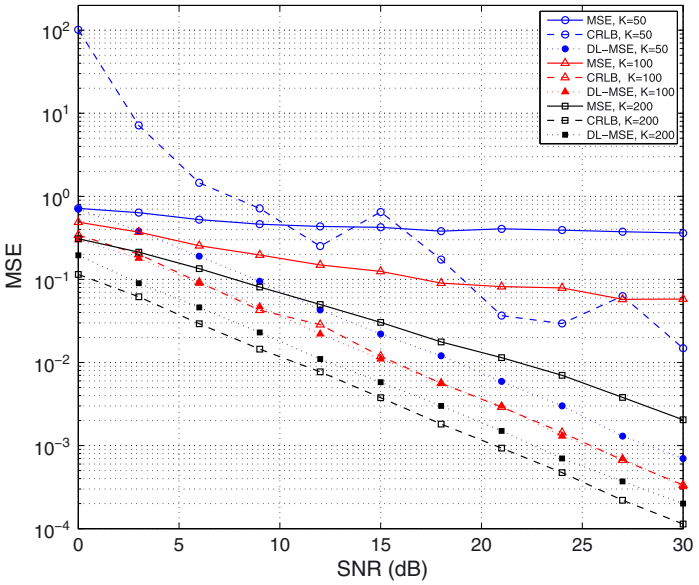

Figure 3. The effect of number of observations K on the mean square error (MSE) performance when $T_c = 100$ ns and $T_s = 0.25$ ns for channel model CM1.

4. RESULTS

In this section, we investigate the effects of IEEE 802.15.4a channel models and the channel resolution on the channel estimation and system performance. For that, we evaluate the MSE of channel estimation and the lower bounds, and the BER performance for various number of observations K and channel resolution values T_s with different channel models. To remove the path loss effect and to treat each channel model fairly, we normalize the channel coefficients as $\sum_{n=1}^{N} \alpha_n^2 = 1$. For the generation of channels, the standardized IEEE 802.15.4a channel models [25] are used.

Initially, in Figure 3, we investigate the effect of number of observations K on the MSE performance when $T_c = 100$ ns and $T_s = 0.25$ ns for the most commonly used channel model CM1. Accordingly, the discrete-time channel length is $N = 400$. Note that the number of nonzero coefficients M may vary for each channel realization generated by its equivalent probabilistic model. Here, K/N can be seen as the ratio of the compressed sampling rate to the conventional receiver sampling rate. As shown in Figure 3, although $K = 50$ observations are not enough for channel estimation even at high SNR, $K = 200$ observations can achieve an MSE $\approx 10^{-2}$ at SNR $= 20$ dB for a fixed $T_s = 0.25$ ns.

In addition to the MSE values, CRLB and the deterministic lower MSE curves are plotted. The first important point for the lower bounds is that if the observations used for CS-based channel estimation are selected as $K = 50$, especially for the low SNR region, the CRLB curve does not provide accurate information. This is mainly due to having insufficient number of observations. Accordingly, the deterministic lower MSE can be used as an approximation, which provides a more reliable bound for insufficient number of observations. The second important point for the lower bounds is that the gap between the MSE and the CRLB curves (and as well as the deterministic lower MSE) becomes smaller as the number of observations increases. Finally, the DL-MSE can be used instead of the CRLB as a lower bound with reduced computational complexity as they show close performances.

In Figure 4, the effect of channel resolution T_s on the MSE performance is investigated when $T_c = 100$ ns and $K/N = 50\%$ for channel model CM1. Hence, the discrete-time channel length is $N = T_c/T_s = \{100, 200, 300, 400, 500\}$ for various channel resolution values. It can be observed that the MSE performance improves with increasing the channel resolution for $K/N = 50\%$ fixed.

DOI: 10.1002/dac

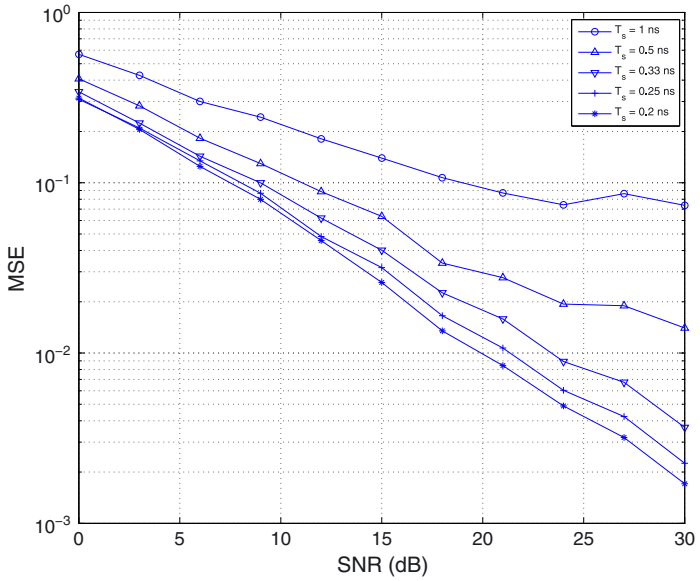

Figure 4. The effect of channel resolution T_s on the mean square error performance when $T_c = 100$ ns and $K/N = 50\%$ for channel model CM1.

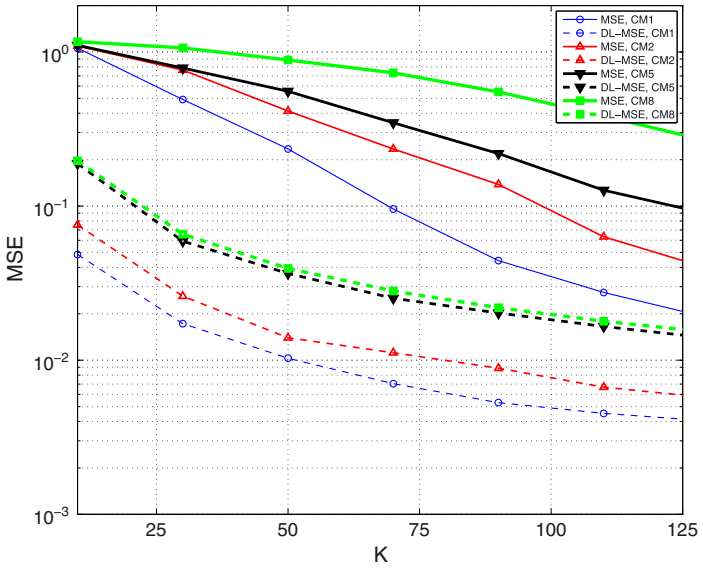

Figure 5. The effect of number of observations K on the mean square error (MSE) performance at SNR = 20 dB when $T_c = 250$ ns and $T_s = 1$ ns for channel models CM1, CM2, CM5, CM8.

It should be noted that for the $T_s = 1$ ns resolution, the MSE $\approx 10^{-1}$ even at high SNR. This shows that the channel model loses its sparse structure for the selected channel resolution.

After considering the most commonly used channel model CM1, let us compare the channel models for the same set of parameters. In Figures 5 and 6, the effect of number of observations K on the MSE and the deterministic lower MSE performances at SNR = 20 dB are investigated when the channel length is $T_c = 250$ ns for channel models CM1, CM2, CM5, and CM8.

The channel resolutions in each figure are $T_s = 1$ ns and $T_s = 0.25$ ns resulting in $N = 250$ and $N = 1000$, respectively. Both figures can be compared with each other fairly based on the K/N ratio. It can be observed that for the same conditions, the channel estimation is better for

DOI: 10.1002/dac

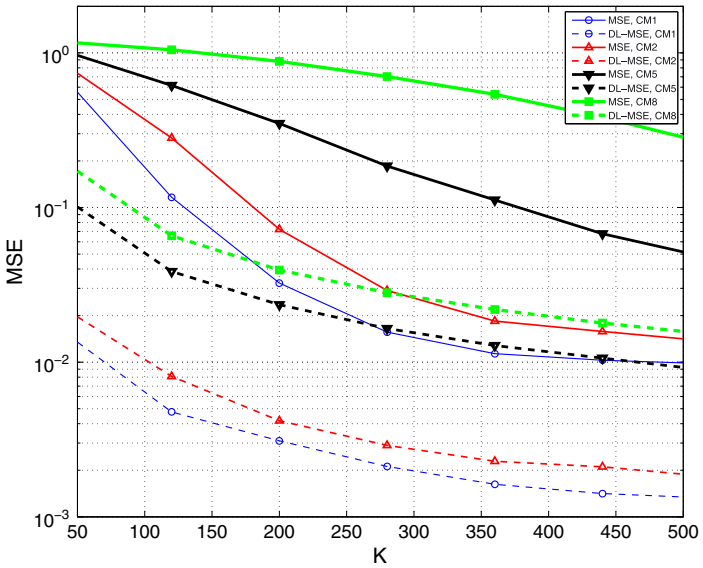

Figure 6. The effect of number of observations K on the mean square error performance at SNR $=$ 20 dB when $T_c = 250$ ns and $T_s = 0.25$ ns for channel models CM1, CM2, CM5, CM8.

channel models in the order of CM1, CM2, CM5, and CM8 as expected. When the channel resolution is increased from $T_s = 1$ ns to $T_s = 0.25$ ns, it can be observed that the MSE performances of CM1, CM2, and CM5 are improved, whereas the performance of CM8 does not change. This can be explained by the dense multipaths arriving almost in each time bin although the resolution is increased (cf. Table II). This is also true for the deterministic lower MSE as the ratio M/K is directly proportional to the sparsity ratio M/N for fixed K and N values. In addition, we can also observe that the MSE performances of CM1 and CM2 do not change much for the resolution $T_s = 0.25$ ns when $400 < K < 500$. Hence, the number of observations can be limited to $K \approx 400$, that is, a lower sampling rate can be used for a similar MSE performance.

Before considering the system performance, we finally investigate the effects of number of observations and channel resolution on the MSE performance for channel model CM5 in the following two figures. Channel model CM5 is selected as the MSE performance of CM2 is similar to that of CM1, and the MSE performance of CM8 does not change much with the channel resolution. In Figure 7, the effect of number of observations K on the MSE performance is investigated when $T_c = 250$ ns and $T_s = 0.25$ ns. Here, the equivalent discrete-time channel length is $N = 1000$. As can be observed, when $K = 250$ observations are used, the MSE performance is poor (i.e., at the rate $K/N = 0.25$). On the other hand, increasing the observations to $K = \{500, 750\}$ improves the MSE at the expense of increasing the compressed sampling rate. In Figure 8, the effect of channel resolution T_s on the MSE performance is investigated when $T_c = 250$ns and $K/N = 50\%$. Hence, the discrete-time channel length is $N = T_c/T_s = \{250, 500, 750, 100, 1250\}$ for various channel resolution values. Similar to the MSE performance for CM1 in Figure 4, the MSE performance improves with increasing the channel resolution for $K/N = 50\%$ fixed. Hence, the sparsity condition of the channel is improved with the channel resolution.

The system performance can be assessed by evaluating the BER performances. We are particularly interested in the low to medium SNR region where typical communication takes place. As for the modulation, binary phase shift keying is used to transmit data. In Figures 9 and 10, the effect of channel resolution on the BER is investigated in CM1 for an all-rake and a partial-rake receiver with five fingers when channel length $T_c = 100$ ns and channel resolutions $T_s = \{0.25, 1\}$ ns are considered for $K/N = 50\%$. BER performances are compared for both perfectly known and estimated channels (PKC, EC). For the partial-rake, it is assumed that the locations of the multipaths are known, whereas the amplitudes are estimated. In Figure 9, when an all-rake receiver is

DOI: 10.1002/dac

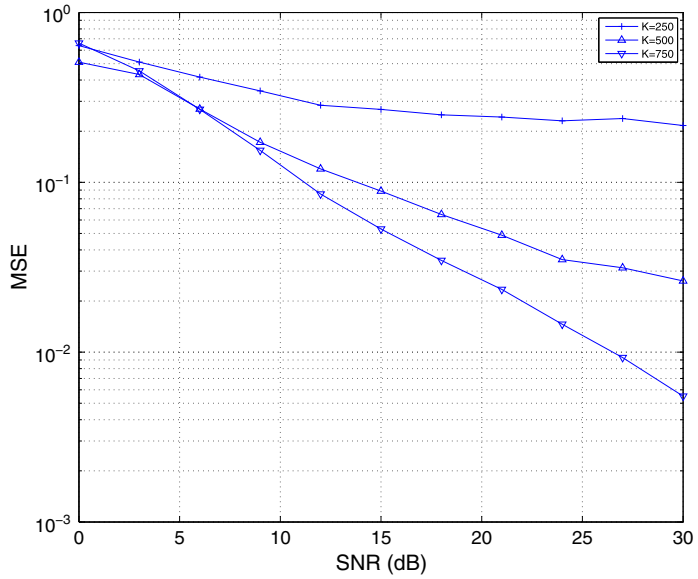

Figure 7. The effect of number of observations K on the mean square error performance when $T_c = 250$ ns and $T_s = 0.25$ ns for channel model CM5.

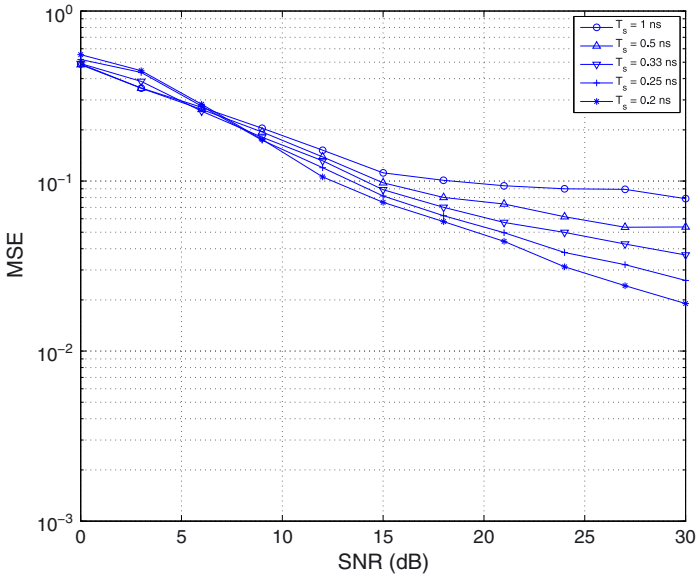

Figure 8. The effect of channel resolution T_s on the mean square error performance when $T_c = 250$ ns and $K/N = 50\%$ for channel model CM5.

used for $T_s = 1$ ns, BER performance for the EC case is worse than the PKC case about 1–2 dB. Correlatively, when a partial-rake receiver with five fingers is used, it can be seen that the relative performance degradation is approximately <1 dB. In Figure 10, it can be observed that with increasing channel resolution to 0.25 ns, the curves of EC and PKC approach each other (i.e., better channel estimation performance) and the BER decreases compared with the former case. For this selected channel resolution, when an all-rake receiver is used, the results for the EC case approach to the PKC case. It is also important that when practical-rake receivers (less fingers) are used, the BER performance curves for EC and PKC become very close to each other as the strongest paths are estimated correctly.

DOI: 10.1002/dac

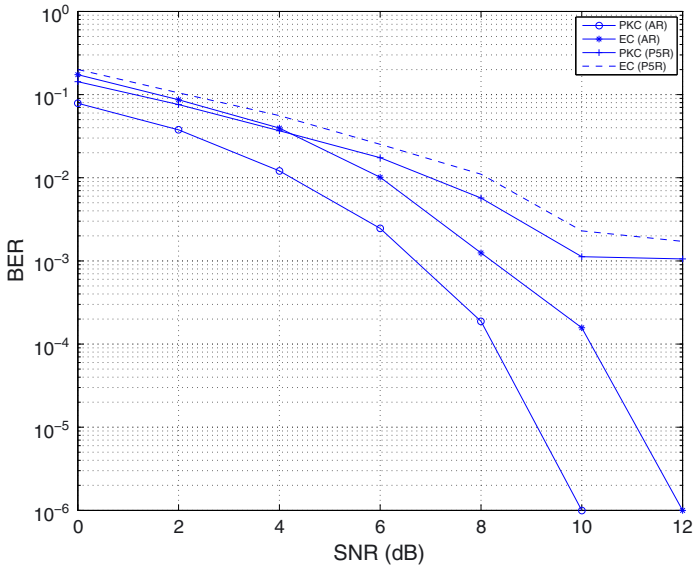

Figure 9. BER performance when $T_s = 1$ ns for channel model CM1.

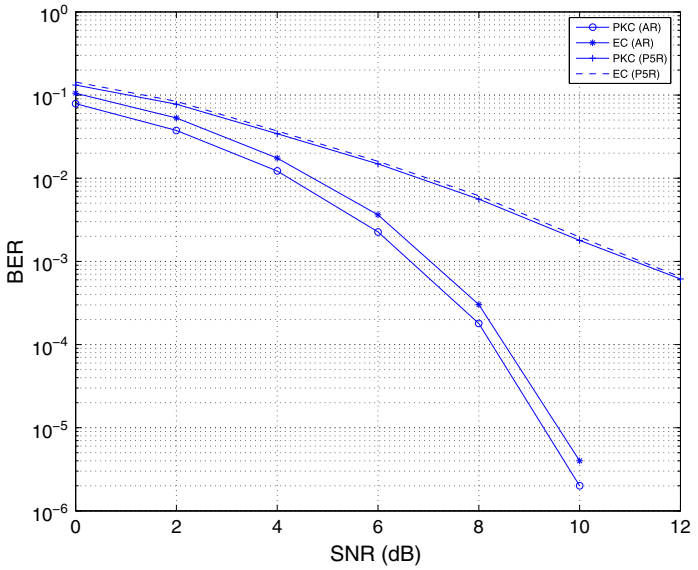

Figure 10. BER performance when $T_s = 0.25$ ns for channel model CM1.

Finally, in Figure 11, we evaluate the BER performance with the estimated and perfectly known channels for various rake receiver implementations when CM1 and CM5 are considered for a fixed channel resolution. For the partial-rake, it is assumed that both the locations and amplitudes of the multipaths are estimated. The channel length and channel resolution are selected as $T_c = 250$ ns and $T_s = 0.25$ ns, respectively, and the sampling ratio, K/N, is fixed to 50%. When an all-rake receiver is used, it can be observed that the BER performances are worse about 0.5 dB and 1 dB for CM1 and CM5, respectively. When a selective-rake receiver with five fingers is used for CM1, the performances for the known and estimated channels are similar as the strongest paths are correctly determined by the CS-based estimation. However, when a partial-rake with five fingers is used for CM1, the BER performance for the estimated channel compared with the known channel has degraded much as the CS-based estimation introduces nonzero components at low SNR, which

DOI: 10.1002/dac

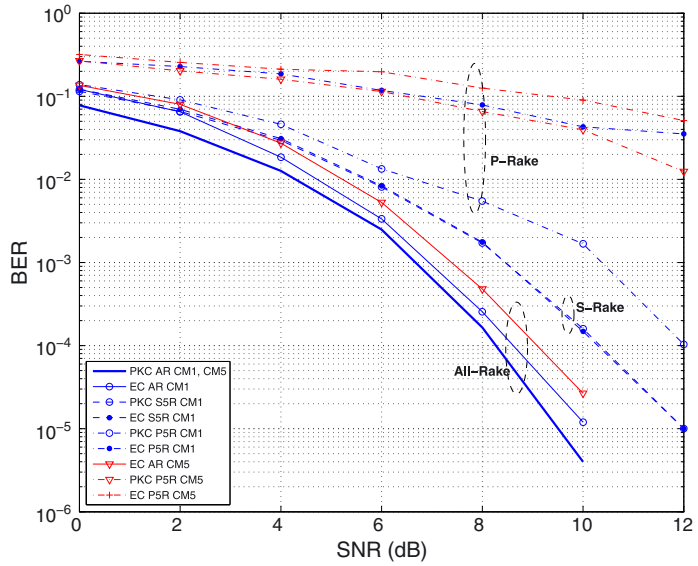

Figure 11. BER performance of various Rake implementations (AR, P5R: partial 5-rake, S5R) for PKC and EC.

are possibly selected as the fingers of a partial-rake. Finally, it can be observed that for CM5, five fingers are not enough to collect significant energy for either known or estimated channels.

Considering the results presented in Figures 3–11 and Table II, CS-based UWB channel estimation can be considered for practical system implementations. For example, for a desired channel estimation performance, pulse widths and number of measurements can be determined for given channel environments. Furthermore, for a desired system performance, type of rake receivers and number of rake fingers can be determined after the CS-based channel estimation. Hence, desired system performances can be achieved depending on the selection of system parameters.

5. CONCLUSIONS

In this study, we investigated the suitability of standardized UWB channel models to be used with the CS theory. In other words, we elaborated on the sparsity assumption of realistic UWB multipath channels. We particularly investigated the effects of (i) IEEE 802.15.4a UWB channel models, which are classified according to the measurement environments, and (ii) selection of channel resolution, which depends on the transmitted pulse width. The channel estimation performance was determined in terms of the MSE of the channel gain estimates, and the BER performance was evaluated with estimated channel parameters for practical rake implementations. Furthermore, CRLB and the deterministic lower MSE were considered. It was shown that UWB channel models for residential environments exhibited a sparse structure yielding a reasonable channel estimation performance, whereas the channel models for industrial environments may not be treated as having a sparse structure due to multipaths arriving densely. Moreover, it was shown that the sparsity increased by channel resolution can improve the channel estimation performance significantly at the expense of increased receiver processing. It was also observed that the use of selective-rake receivers after CS-based sparse channel estimation yields a BER performance very close to the known channel case. The results of this study are important for the practical implementation of the CS theory to UWB channel estimation.

ACKNOWLEDGEMENT

This work was supported in part by The Scientific and Technological Research Council of Turkey (TUBITAK) under grant no. 108E054.

DOI: 10.1002/dac

REFERENCES

1. Win MZ, Scholtz RA. Ultra-wide bandwidth time-hopping spread-spectrum impulse radio for wireless multiple-access communications. *IEEE Transactions on Communications* 2000; **48**:679–691.
2. IEEE Std 802.15.4a-2007: Part 15.4: Wireless Medium Access Control (MAC) and Physical Layer (PHY) Specifications for Low-Rate Wireless Personal Area Networks (WPANs), 2007.
3. Lie JP, Ng BP, See CMS. Direction finding receiver for UWB impulse radio signal in multipath environment. *International Journal of Communication Systems* 2010; **23**:1537–1553. DOI: 10.1002/dac.1123.
4. Zeinalpour-Yazdi Z, Nasiri-Kenari M, Aazhang B. Performance of UWB linked relay network with time-reversed transmission in the presence of channel estimation error. *IEEE Transactions on Wireless Communications* 2012; **11**:2958–2969.
5. Liao S-H, Chiu C-C, Ho M-H, Liu C-L. Channel capacity of multiple-input multiple-output ultra-wideband systems with single co-channel interference. *International Journal of Communication Systems* 2010; **23**:1600–1612. DOI: 10.1002/dac.1131.
6. Abbasi-Moghadam D, Vakili VT. Characterization of indoor time reversal UWB communication systems: Spatial, temporal and frequency properties. *International Journal of Communication Systems* 2011; **24**:277–294. DOI: 10.1002/dac.1140.
7. Liang Z, Jin L, Dong X. Downlink multiple access schemes for transmitted reference pulse cluster UWB systems. *International Journal of Communication Systems* 2011; **24**:732–744. DOI: 10.1002/dac.1180.
8. Lottici V, D'Andrea A, Mengali U. Channel estimation for ultra-wideband communications. *IEEE Journal on Selected Areas in Communications* 2002; **20**:1638–1645.
9. Huang L, Ko CC. Performance of maximum-likelihood channel estimator for UWB communications. *IEEE Communications Letters* 2004; **8**:356–358.
10. Candes EJ, Romberg J, Tao T. Robust uncertainty principles: exact signal reconstruction from highly incomplete frequency information. *IEEE Transactions on Information Theory* 2006; **52**:489–509.
11. Donoho D. Compressed sensing. *IEEE Transactions on Information Theory* 2006; **52**:1289–1306.
12. Bajwa WU, Haupt J, Sayeed AM, Nowak R. Compressed channel sensing: a new approach to estimating sparse multipath channels. *IEEE Communications Magazine* 2010; **98**:1058–1076.
13. Berger CR, Wang Z, Huang J, Zhou S. Application of compressive sensing to sparse channel estimation. *IEEE Communications Magazine* 2010; **48**:164–174.
14. Lampe L, Witrisal K. Challenges and recent advances in IR-UWB system design. *IEEE Proceedings– ICUWB: International Conference on Ultra Wideband*, Nanjing, China, 20-23 September 2010; 3288–3291.
15. Yang D, Li H, Peterson GD, Fathy A. Compressed sensing based UWB receiver: hardware compressing and FPGA reconstruction. *IEEE Proceedings–CISS: Annual Conference on Information Sciences and Systems*, Baltimore, MD, USA, 18-20 March 2009; 198–201.
16. Oka A, Lampe L. A compressed sensing receiver for bursty communication with UWB impulse radio. *IEEE Proceedings–ICUWB: International Conference on Ultra Wideband*, Vancouver, Canada, 9-11 September 2009; 279–284.
17. Zhang P, Hu Z, Qiu RC, Sadler BM. A compressed sensing based ultra-wideband communication system. *IEEE Proceedings–ICC: International Conference on Communications*, Dresden, Germany, 14-18 June 2009; 1–5.
18. Paredes JL, Arce GR, Wang Z. Ultra-wideband compressed sensing: channel estimation. *IEEE Journal of Selected Topics in Signal Processing* 2007; **1**:383–395.
19. Liu TC-K, Dong X, Lu W-S. Compressed sensing maximum likelihood channel estimation for ultra-wideband impulse radio. *IEEE Proceedings–ICC: International Conference on Communications*, Dresden, Germany, 14-18 June 2009; 1–5.
20. Naini FM, Gribonval R, Jacques L, Vandergheynst P. Compressive sampling of pulse trains: spread the spectrum. *IEEE Proceedings–ICASSP: International Conference on Acoustics, Speech and Signal Processing*, Taipei, Taiwan, 19-24 April 2009; 2877–2880.
21. Yu H, Guo S. Pre-filtering ultra-wideband channel estimation based on compressed sensing. *IEEE Proceedings–CMC: International Conference on Communications and Mobile Computing*, Shenzen, China, 12-14 April 2010; 110–114.
22. Jian C, Ye X, Zhu W-P. Improved compressed sensing-based UWB channel estimation. *Proceedings–WCSP: International Conference on Wireless Communications and Signal Processing*, Nanjing, China, 9-11 November 2011; 1–5.
23. Barbieri A, Pancaldi F, Vitetta GM. Compressed channel estimation and data detection algorithms for IR-UWB. *IEEE Proceedings ICUWB: International Conference on Ultra Wideband*, Bologna, Italy, 14-16 September 2011; 360–364.
24. Lagunas E, Najar M. Sparse channel estimation based on compressed sensing for ultra wideband systems. *IEEE Proceedings ICUWB: International Conference on Ultra Wideband*, Bologna, Italy, 14-16 September 2011; 365–369.
25. Molisch AF, Cassioli D, Chong CC, Emami S, Fort A, Kannon B, Karedal J, Kunisch J, Schantz HG, Siwiak K, Win MZ. A comprehensive standardized model for ultrawideband propagation channels. *IEEE Transactions on Antennas and Propagation* 2006; **54**:3151–3166.
26. Erküçük S, Kim DI, Kwak KS. Effects of channel models and rake receiving process on UWB-IR system performance. *IEEE Proceedings ICC: International Conference on Communications*, Glasgow, Scotland, 24-28 June 2007; 4896–4901.

27. Candes EJ, Wakin MB. An Introduction to compressive sampling. *IEEE Signal Processing Magazine* 2008; **25**:21–30.
28. ℓ_1-Magic: Recovery of Sparse Signals via Convex Programming. (Available from: [http://users.ece.gatech.edu/justin/l1magic/downloads/l1magic.pdf]).
29. Carbonelli C, Vedantam S, Mitra U. Sparse channel estimation with zero tap detection. *IEEE Transactions on Wireless Communications* 2007; **6**:1743–1763.
30. Raz G, Bajwa WU, Haupt J, Nowak R. Compressed channel sensing. *IEEE Proceedings CISS: Annual Conference on Information Sciences and Systems*, Princeton, NJ, USA, 19-21 March 2008; 5–10.

AUTHORS' BIOGRAPHIES

Mehmet Başaran received the B.Sc. and M.Sc. degrees in Electrical and Electronics Engineering from Istanbul University, Turkey in 2008 and 2011, respectively. Currently he is pursuing his Ph.D. degree in Telecommunication Engineering and working as a research and teaching assistant at Istanbul Technical University. His current research areas include wireless communications, cognitive radio networks, energy-efficient (green) and UWB communication systems.

Serhat Erküçük received the B.Sc. and M.Sc. degrees in Electrical Engineering from Middle East Technical University, Ankara, Turkey and from Ryerson University, Toronto, ON, Canada, in 2001 and 2003, respectively, and the Ph.D. degree in Engineering Science from Simon Fraser University, Burnaby, BC, Canada in 2007. He was an NSERC postdoctoral fellow at the University of British Columbia, Vancouver, BC, Canada before joining Kadir Has University, Istanbul, Turkey as an assistant professor in 2008. His research interests are in physical layer design of emerging communication systems, wireless sensor networks and communication theory. Dr. Erküçük serves as an area editor for AEÜ – International Journal of Electronics and Communications.

Hakan Ali Çırpan received the B.S. degree in 1989 from Uludag University, Bursa, Turkey, the M.S. degree in 1992 from the University of Istanbul, Istanbul, Turkey, and the Ph.D. degree in 1997 from the Stevens Institute of Technology, Hoboken, NJ, USA, all in electrical engineering. From 1995 to 1997, he was a Research Assistant with the Stevens Institute of Technology, working on signal processing algorithms for wireless communication systems. In 1997, he joined the faculty of the Department of Electrical-Electronics Engineering at The University of Istanbul. In 2010 he has joined to the faculty of the department of Electronics & Communication Engineering at Istanbul Technical University. His general research interests cover wireless communications, statistical signal and array processing, system identification and estimation theory. His current research activities are focused on machine learning, signal processing and communication concepts with specific attention to channel estimation and equalization algorithms for future wireless systems.

DOI: 10.1002/dac